

## Research Article

# Mathematical Modeling and Analysis on the Effects of Surgery and Chemotherapy on Lung Cancer

Md. Ahsan Ullah and Uzzwal Kumar Mallick 

*Mathematics Discipline, Khulna University, Khulna 9208, Bangladesh*

Correspondence should be addressed to Uzzwal Kumar Mallick; [mallickuzzwal@math.ku.ac.bd](mailto:mallickuzzwal@math.ku.ac.bd)

Received 27 April 2023; Revised 18 May 2023; Accepted 6 June 2023; Published 23 June 2023

Academic Editor: Waleed Adel

Copyright © 2023 Md. Ahsan Ullah and Uzzwal Kumar Mallick. This is an open access article distributed under the Creative Commons Attribution License, which permits unrestricted use, distribution, and reproduction in any medium, provided the original work is properly cited.

Lung cancer is the biggest cause of cancer mortality worldwide and a major impediment to extending life expectancy. In comparison to other cancers, it has a relatively poor survival rate. In this paper, we have developed a mathematical model for lung cancer based on biological phenomena using nonlinear ordinary differential equations and analyzed it both analytically and numerically. According to the findings, CD8+ T cells and dendritic cells have a role in tumor cell variety. Surgery and chemotherapy have been used as treatment options, and we have observed that three doses of chemotherapy after surgery had the greatest results after examining several treatment options. During the treatment period, the cycle of each chemotherapy has been taken every 4 weeks, and the first dose has been taken after 28 days of surgery. Finally, we have evaluated the various starting dates for the best treatment choice and discovered that the patient who begins treatment sooner has a better probability of surviving.

## 1. Introduction

More than AIDS, TB, and malaria combined, cancer kills one out of every six people on the planet. It is now the world's second biggest cause of mortality, particularly in nations with a high or extremely high Human Development Index (HDI) [1]. Because of rising life expectancy and epidemiological and demographic shifts, the number of new cases and fatalities continues to climb. By 2030, SDG 3.4 asks for a one-third decrease in noncommunicable disease (NCD) related premature mortality. Unfortunately, improvement in cancer has lagged behind advances in other NCDs. There were an estimated 18.1 million new cancer diagnoses and 9.6 million cancer deaths in 2018. The incidence rate of cancer was 48.4%, 21.0%, 23.4%, 5.8%, and 1.4% in Asia, the Americas, Europe, Africa, and Oceania, respectively [2].

Among all cancer types, lung cancer is one of the main causes of cancer mortality, accounting for over 25% of all cancer fatalities which kills more people than colon, breast, and prostate cancers combined [3]. In 2018, lung cancer was one of the most diagnosed malignancies in very high HDI and medium HDI countries among men [1]. This type of cancer was found to be prevalent in 13.1 percent of men and 2% of

females in Bangladesh during the previous five years [4]. According to the World Health Organization, the overall number of cancer patients in Bangladesh was 150,781 in 2018, with 108,137 deaths. Lung cancer afflicted 8.2 percent of the cancer patients, with a mortality rate of 11%. WHO said that the number of cases of lung cancer in 2012 was 10,851 and 12,374 in 2018, and 26,738 cases are expected in 2040. Compared to breast cancer, lung cancer will be a more dangerous kind of cancer in 2040 [5].

For investigating cancer dynamics, many studies have been done. A mathematical model of cancer progression was devised by de Pillis et al. [6]. They used a combination of chemotherapy and activated antitumor cell transfer (TIL injections) and activation protein injections (IL-2 injections) to treat the patients. In order to comprehend the dynamics of immune-mediated tumor rejection, de Pillis et al. [7] also provided a novel mathematical model that depicts tumor-immune interactions, concentrating on the function of natural killer (NK) and CD8+ T cells in tumor surveillance. Trisilowati et al. [8] proposed a mathematical model in which they have taken natural killer, cytotoxic T lymphocytes, and dendritic cells as immune cells and employed dendritic cells

to treat patients. Motivated by both of them, Unni and Seshaiyer [9] develop a mathematical model in which he discussed the interactions between tumor cells and immune cells including CD8+ T cells, natural killer cells, and dendritic cells combined with drug delivery to these cell sites.

Kirschner and Tsygvintsev [10] presented a new form of tumor therapy and built a mathematical model that predicted tumor immune responses. This therapeutic method employs elements of the host to increase the immune response in the hopes of allowing the tumor to be cleared. After that work, Kirschner and Panetta [11] use mathematical modeling to describe the interplay between tumor cells, immune-effector cells, and IL-2. Both short-term tumor growth fluctuations and long-term tumor relapse might be explained by these efforts. The researchers next looked at how adoptive cellular immunotherapy affected the mouse and defined the situations under which the tumor may be destroyed.

Decker et al. [12] looked through the literature to find and characterize the turning points in immunotherapy's approval as a legitimate therapeutic option for neoplastic malignancy. In mice and dogs, they also concentrate on research milestones and the establishment of essential model systems. By following this work, Waldman et al. [13] gave a thorough historical and biological overview of the development and clinical application of cancer immunotherapeutic, emphasizing the fundamental importance of T lymphocyte regulation and highlighting clinical trials that demonstrate therapeutic efficacy and side effects associated with each drug class. Also, an overview of what is currently known about systemic immunity in cancer was provided by Hiam-Galvez et al. [14].

Kartono [15] created a mathematical model that illustrates how interleukin-2 (IL-2), interferon-alpha, and tumor-infiltrating lymphocytes (TIL) affect the dynamics of tumor cells. McLane et al. [16] discussed the understanding of the biology of Tex cells, including the developmental pathways, transcriptional and epigenetic characteristics, and intrinsic and extrinsic factors affecting cell exhaustion. Philip and Schietinger [17] discussed the present state of knowledge on the factors that affect T cells' receptivity to and resistance to immunotherapy, and they highlighted unanswered research topics.

The study by Casiraghi et al. [18] was conducted in a single center and used patients who had been treated over the previous 20 years. It was up to date with all the current staging systems and used a multimodality approach to reduce group heterogeneity and better identify potential prognostic factors for the best patient selection. Using SCLC patients who had chemotherapy, Liang et al. [19] aimed to create a predictive nomogram in their study. Chao et al. [20] conducted an investigation and developed a prediction algorithm to find people who might benefit from surgery. By concentrating primarily on complex mutations that comprise both a common mutation and an unusual mutation, Li et al. [21] retrospectively examined 18 patients with NSCLC who had complex EGFR mutations.

However, there are several models that explain the effects of various immune cells on tumor cells, but only a few models that investigate the effects of dendritic cells on tumor cells. Also, they did not discuss surgery as a treatment option, but we are using both surgery and chemotherapy for our treat-

ment. Additionally, previous authors did not explain the ideal moment to begin this period of treatment. In this regard, our work differs from that of the earlier authors since we developed a mathematical model on non-small-cell lung cancer that includes chemotherapy and surgery into account as possible treatment options and demonstrated the combined impact of these treatment approaches. Moreover, we have recommended the best treatment strategy out of all possible combinations of surgery and various chemotherapy dosages. Finally, we have suggested a time frame within which a patient should begin receiving treatment in order to improve his prognosis.

## 2. Formulation of the Mathematical Model for Lung Cancer

Lung cancer is a cancer that starts in the lungs. When a person has lung cancer, they have abnormal cells that cluster together to form a tumor. Unlike normal cells, cancer cells grow without order or control, destroying the healthy lung tissue around them. These types of tumors are called malignant tumors.

Tumor cells grow logistically and interact to damage the CD8+ T cells while dendritic cells are being activated to mature for the presence of tumor cells. So, a mathematical model is developed based on the Lotka-Volterra and the logistic model. Here, the model consists of three variables such as tumor cells, CD8+ T cells, and dendritic cells, which are denoted by  $T(t)$ ,  $C(t)$ , and  $D(t)$ , respectively.

When tumor cells interact with CD8+ T cells, some tumor cells are killed by CD8+ T cells. Again, in the contact of tumor cells and dendritic cells, dendritic cells destroy some tumor cells. The following nonlinear differential equations are written based on the aforementioned information:

$$\frac{dT}{dt} = \alpha T(1 - \beta T) - \gamma T - \phi CT, \quad (1)$$

where the term  $\alpha T(1 - \beta T)$  represents the logistic growth of tumor,  $\gamma$  is the constant destroying rate of tumor cells because of dendritic cells, and the rate at which CD8+ T cells kill tumor cells is  $\phi$ .

The interacting impact of tumor cells on CD8+ T cells is some of CD8+ T cells are killed by tumor cells. Moreover, because of contact between dendritic cells and tumor cells, some CD8+ T cells are excited. This can be written mathematically as follows:

$$\frac{dC}{dt} = \nu T - \eta CT - \kappa C. \quad (2)$$

Here, the activation rate of CD8+ T cells owing to contact between dendritic cells and tumor cells is indicated by constant rate  $\nu$ ,  $\eta$  is the inactivation rate of CD8+ T cells by tumor cells, and  $\kappa$  is the natural death rate of CD8+ T cells.

Dendritic cells are immature initially, generated by hematopoietic bone marrow progenitor cells. They are found throughout the body under normal circumstances. Because of contacting tumor cells, they become activated matured cells. Then, by activating CD8+ T cells, some dendritic cells become inactive.

$$\frac{dD}{dt} = \mu + \sigma DT - \rho CD - \omega D. \tag{3}$$

The sources of generating dendritic cells are denominated by  $\mu$ , the rate of recruitment of dendritic cells by tumor cells is  $\sigma$ ,  $\rho$  is the rate at which dendritic cells are inactivated by CD8+ T cells, and natural death rate of dendritic cells is betokened by  $\omega$ .

2.1. Mathematical Analysis

2.1.1. Positivity and Boundedness

**Lemma 1.** *Considering  $T(0) > 0$ ,  $C > 0$ , and  $D(0) > 0$ , it must be proved that  $T(t)$ ,  $C(t)$ , and  $D(t)$  will be positive for all  $t \in [0, T_1]$  in  $R_+^3$  where  $T_1 > 0$ .*

*Proof.* Taking all parameters of the system and all initial values to be positive, we have to prove that  $T(t)$ ,  $C(t)$ , and  $D(t)$  will be positive for all  $t \in [0, T]$  in  $R_+^3$ .

From equation (1), we have

$$\begin{aligned} \frac{dT}{dt} &= \alpha T(1 - \beta T) - \gamma T - \phi CT \Rightarrow \frac{dT}{dt} \\ &= T(\alpha - \alpha\beta T - \gamma - \phi C) \Rightarrow \frac{1}{T} \frac{dT}{dt} \\ &= \alpha - \alpha\beta T - \gamma - \phi C. \end{aligned} \tag{4}$$

Integrating both sides of the above equation, we obtain

$$T(t) = e^{\alpha t - \alpha\beta \int T dt - \gamma t - \phi \int C dt} > 0. \tag{5}$$

Therefore,  $T(t) > 0$ .

Equation (2) is given as follows:

$$\frac{dC}{dt} = \nu T - \eta CT - \kappa C \Rightarrow \frac{dC}{dt} > -\eta CT - \kappa C \Rightarrow C > e^{-\kappa t - \eta \int T dt} > 0. \tag{6}$$

So,  $C(t) > 0$ .

Again, from equation (3), we already have,

$$\begin{aligned} \frac{dD}{dt} &= \mu + \sigma DT - \rho CD - \omega D \Rightarrow \frac{dD}{dt} > \sigma DT - \rho CD - \omega D \\ &> e^{\int T dt - \omega t - \rho \int C dt} > 0. \end{aligned} \tag{7}$$

So,  $D(t) > 0$ .

Hence, it can be said that  $T(t)$ ,  $C(t)$ , and  $D(t)$  will be positive for all  $t \in [0, T]$  in  $R_+^3$ . □

**Lemma 2.** *All solutions  $(T(t), C(t), D(t))$  of the system are bounded.*

*Proof.* The constraints used in this system are positive. We define the function

$$P(t) = T(t) + C(t) + D(t). \tag{8}$$

□

The derivative of this equation is

$$\begin{aligned} \frac{dP}{dt} &= \frac{dT}{dt} + \frac{dC}{dt} + \frac{dD}{dt} \Rightarrow \frac{dP}{dt} = \alpha T(1 - \beta T) - \gamma T - \phi CT \\ &+ \nu T - \eta CT - \kappa C + \mu + \sigma DT - \rho CD - \omega D \Rightarrow \frac{dP}{dt} \\ &+ \mu_1 P = \alpha T(1 - \beta T) - \gamma T - \phi CT + \nu T - \eta CT \\ &- \kappa C + \mu + \sigma DT - \rho CD - \omega D + \mu_1(T + C + D). \end{aligned} \tag{9}$$

Now we are taking a function of  $g(x, y, z)$  as follows:

$$\begin{aligned} g(x, y, z) &= \alpha x(1 - \beta x) - \gamma x - \phi xy + \nu x - \eta yx - \kappa y + \mu \\ &+ \sigma zx - \rho yz - \omega z + \mu_1(x + y + z), \end{aligned} \tag{10}$$

where  $(x, y, z)$  is the critical point.

Now, let  $D = 3g_{xx}g_{yy}g_{zz} - g_{xx}g_{yz}^2 - g_{xy}^2g_{zz} - g_{zx}^2g_{yy}$ .

Substituting  $g_{xx} = -2\alpha\beta$ ,  $g_{yy} = 0$ ,  $g_{zz} = 0$ ,  $g_{xy} = -\phi - \eta$ ,  $g_{yz} = -\rho$ , and  $g_{zx} = -\sigma$ , we obtain

$$D = 2\alpha\beta\rho^2 > 0. \tag{11}$$

Since  $D > 0$  and  $g_{xx} < 0$  with  $g_{yy} = 0$ ,  $g_{zz} = 0$ ,  $g(x, y, z)$  has a local maximum. So, considering the maximum value  $M$ , equation (9) implies that

$$\frac{dP}{dt} + \mu_1 P \leq M. \tag{12}$$

Taking the limit supremum, we obtain

$$\lim_{t \rightarrow \infty} \sup P(t) \leq \frac{M}{\mu_1}. \tag{13}$$

All solutions  $(T(t), C(t), D(t))$  of the system are bounded.

2.1.2. Existence and Uniqueness of the Solution

**Lemma 3.** *For all nonnegative initial conditions, the solutions of the system exist, and they are also unique at the same time for all time  $t > 0$ .*

*Proof.* For the existence and uniqueness of a solution indicated by the proposed theorem [22], the Lipschitz criteria

have been chosen as the standard. It must be shown that the system's partial derivative exists and is continuous to qualify for our model to work. Consider

$$\begin{aligned} f(T, C, D) &= \frac{dT}{dt} = \alpha T(1 - \beta T) - \gamma T - \phi CT, \\ g(T, C, D) &= \frac{dC}{dt} = \nu T - \eta CT - \kappa C, \\ h(T, C, D) &= \frac{dD}{dt} = \mu + \sigma DT - \rho CD - \omega D. \end{aligned} \quad (14)$$

The partial derivatives of  $f$ ,  $g$ , and  $h$  with respect to compartments  $T$ ,  $C$ , and  $D$  are calculated as follows using the system's equation described above:

$$\begin{aligned} \frac{\partial f}{\partial T} &= -\gamma - \phi C - \alpha(\beta T - 1) - \alpha\beta T, \left| \frac{\partial f}{\partial T} \right| \\ &= -\gamma - \phi C - \alpha(\beta T - 1) - \alpha\beta T \leq \frac{M}{\mu_1} < \infty, \\ \frac{\partial f}{\partial C} &= -\phi T, \left| \frac{\partial f}{\partial C} \right| = \phi T \leq \frac{M}{\mu_1} < \infty, \\ \frac{\partial f}{\partial D} &= 0, \left| \frac{\partial f}{\partial D} \right| = 0 \leq \frac{M}{\mu_1} < \infty. \end{aligned} \quad (15)$$

Again,

$$\begin{aligned} \frac{\partial g}{\partial T} &= \nu - \eta C, \left| \frac{\partial g}{\partial T} \right| = -\nu + \eta C \leq \frac{M}{\mu_1} < \infty, \\ \frac{\partial g}{\partial C} &= -\kappa - \eta T, \left| \frac{\partial g}{\partial C} \right| = \kappa + \eta T \leq \frac{M}{\mu_1} < \infty, \\ \frac{\partial g}{\partial D} &= 0, \left| \frac{\partial g}{\partial D} \right| = 0 \leq \frac{M}{\mu_1} < \infty. \end{aligned} \quad (16)$$

Lastly,

$$\begin{aligned} \frac{\partial h}{\partial T} &= \sigma D, \left| \frac{\partial h}{\partial T} \right| = \sigma D \leq \frac{M}{\mu_1} < \infty, \\ \frac{\partial h}{\partial C} &= -\rho D, \left| \frac{\partial h}{\partial C} \right| = \rho D \leq \frac{M}{\mu_1} < \infty, \\ \frac{\partial h}{\partial D} &= \sigma T - \omega - \rho C, \left| \frac{\partial h}{\partial D} \right| = -\sigma T + \omega + \rho C \leq \frac{M}{\mu_1} < \infty. \end{aligned} \quad (17)$$

The associated theorem establishes that  $T$ ,  $C$ , and  $D$  are locally continuous in  $R_3^+$  and have a unique solution since all partial derivatives exist and are continuous.  $\square$

**2.1.3. Equilibrium Analysis.** By solving the following equations below, we can obtain equilibrium point

$$\alpha T(1 - \beta T) - \gamma T - \phi CT = 0, \quad (18)$$

$$\nu T - \eta CT - \kappa C = 0, \quad (19)$$

$$\mu + \sigma DT - \rho CD - \omega D = 0. \quad (20)$$

Solving equations (18)-(20), we get two equilibrium points  $E_0(0, 0, \mu/\omega)$  and  $E_1(T^*, C^*, D^*)$ , where

$$\begin{aligned} T^* &= \frac{\alpha - \gamma - \phi C^*}{\alpha\beta}, \\ C^* &= \frac{-(\eta\gamma - \eta\alpha - \phi\nu - \kappa\alpha\beta) \pm \sqrt{(\eta\gamma - \eta\alpha - \phi\nu - \kappa\alpha\beta)^2 - 4(\eta\phi)\nu(\alpha - \beta)}}{2\eta\phi}, \\ D^* &= \frac{\mu}{\rho C^* - \sigma T^* + \omega}. \end{aligned} \quad (21)$$

**2.1.4. Basic Reproduction Number.** For investing basic reproduction number  $R_0$ , we will use next generation matrix method [23, 24]. From our mathematical model, it is clear that the only relevant class of infected cells is tumor cells  $T(t)$ . We have

$$\frac{dT}{dt} = \alpha T(1 - \beta T) - \gamma T - \phi CT. \quad (22)$$

Differentiating the above equation with respect to  $T$ , we have

$$\frac{d}{dT} \left( \frac{dT}{dt} \right) = -\gamma - \phi C - \alpha(\beta T - 1) - \alpha\beta T. \quad (23)$$

At the equilibrium point  $(T^*, C^*, \text{ and } D^*)$ , we obtain

$$\frac{d}{dT} \left( \frac{dT}{dt} \right) = -\gamma - \phi C^* - \alpha(\beta T^* - 1) - \alpha\beta T^*. \quad (24)$$

Therefore, two matrices  $F$  and  $V$  which represent the gain and loss of tumor cells are  $F = \alpha$  and  $V = 2\alpha\beta T + \gamma + \phi C$ . Then, the basic reproduction number is the largest eigenvalue of  $FV^{-1}$ . Therefore, we have

$$R_0 = \frac{F}{V} = \frac{\alpha}{2\alpha\beta T^* + \gamma + \phi C^*}. \quad (25)$$

This fundamental reproduction number indicates that tumor cells will disappear from the human body if  $\alpha < 2\alpha\beta T^* + \gamma + \phi C^*$  and that they will persist if  $\alpha > 2\alpha\beta T^* + \gamma + \phi C^*$ .

**2.1.5. Stability Analysis of the System at the Equilibrium Point.** The Jacobian matrix will be used, and then, the characteristic equation will be analyzed for investigating the behavior of the stability.

**Theorem 4.** *The equilibrium point  $E_0$  is asymptotically stable if  $\gamma > \alpha$ .*

*Proof.* To prove Theorem 4, at first, we consider

$$f = \alpha T(1 - \beta T) - \gamma T - \phi CT, \quad (26)$$

$$g = \nu T - \eta CT - \kappa C, \quad (27)$$

$$h = \mu + \sigma DT - \rho CD - \omega D. \quad (28)$$

For equations (26) to (28), the Jacobian matrix is

$$J = \frac{\partial(f, g, h)}{\partial(T, C, D)} = \begin{bmatrix} \frac{\partial f}{\partial T} & \frac{\partial f}{\partial C} & \frac{\partial f}{\partial D} \\ \frac{\partial g}{\partial T} & \frac{\partial g}{\partial C} & \frac{\partial g}{\partial D} \\ \frac{\partial h}{\partial T} & \frac{\partial h}{\partial C} & \frac{\partial h}{\partial D} \end{bmatrix} \Rightarrow J = \begin{bmatrix} -\gamma - \phi C - \alpha(\beta T - 1) - \alpha\beta T & -\phi T & 0 \\ \nu - \eta C & -\kappa - \eta T & 0 \\ \sigma D & -\rho D & \sigma T - \omega - \rho C \end{bmatrix}. \tag{29}$$

At the equilibrium point  $E_0(0, 0, \mu/\omega)$ , equation (29) becomes

$$J = \begin{bmatrix} \alpha - \gamma & 0 & 0 \\ \nu & -\kappa & 0 \\ \frac{\mu\sigma}{\omega} & -\frac{\mu\rho}{\omega} & -\omega \end{bmatrix}. \tag{30}$$

The characteristic equation is

$$\begin{aligned} &-(\kappa + \lambda)(\omega + \lambda)(\gamma - \alpha + \lambda) = 0, \\ &\Rightarrow (\kappa + \lambda)(\omega + \lambda)(\gamma - \alpha + \lambda) = 0, \\ &\Rightarrow \lambda^3 + \lambda^2(\kappa + \omega + \gamma - \alpha) + \lambda(\omega\gamma - \omega\alpha - \kappa\alpha + \kappa\gamma + \kappa\omega) \\ &\quad + \kappa\omega(\gamma - \alpha) = 0, \end{aligned}$$

$$\Rightarrow \beta_0\lambda^3 + \beta_1\lambda^2 + \beta_2\lambda + \beta_3 = 0, \tag{31}$$

where

$$\begin{aligned} \beta_0 &= 1, \\ \beta_1 &= \kappa + \omega + \gamma - \alpha, \\ \beta_2 &= \omega\gamma - \omega\alpha - \kappa\alpha + \kappa\gamma + \kappa\omega, \\ \beta_3 &= \kappa\omega(\gamma - \alpha). \end{aligned} \tag{32}$$

Now,

$$\begin{aligned} \beta_1\beta_2 - \beta_3 &= 2\kappa\omega(\gamma - \alpha) + \kappa^2(\gamma - \alpha) + \omega^2(\gamma - \alpha) + \kappa^2\omega \\ &\quad + \omega^2\kappa + (\omega + \kappa)(\gamma - \alpha)^2. \end{aligned} \tag{33}$$

It is clear that, if  $\gamma > \alpha$ , then  $\beta_1 > 0$ ,  $\beta_2 > 0$ , and  $\beta_1\beta_2 - \beta_3 > 0$ . So, according to the Routh-Hurwitz stability criterion, the equilibrium point  $E_0(0, 0, \mu/\omega)$  is asymptotically stable.  $\square$

Alternatively, at the equilibrium point  $E_0(0, 0, \mu/\omega)$ , we have basic reproduction number  $R_0 = \alpha/\gamma$ . First two eigenvalues are negative, and third one is  $\lambda = \alpha - \gamma \Rightarrow \lambda = \gamma(\alpha/\gamma - 1) \Rightarrow \lambda = \gamma(R_0 - 1)$ . This eigenvalue is negative if  $R_0 < 1$ , and the system will be stable at the equilibrium point  $E_0(0, 0, \mu/\omega)$ .

**Theorem 5.** *The equilibrium point  $E_1(T^*, C^*, D^*)$  is stable if  $\gamma > \alpha$  and  $\omega + \rho C^* > \sigma T^*$ .*

*Proof.* The Jacobian matrix at the equilibrium point  $(T^*, C^*, D^*)$  is

$$\begin{aligned} J(T^*, C^*, D^*) &= \begin{bmatrix} \frac{\partial f(T^*, C^*, D^*)}{\partial T^*} & \frac{\partial f(T^*, C^*, D^*)}{\partial C^*} & \frac{\partial f(T^*, C^*, D^*)}{\partial D^*} \\ \frac{\partial g(T^*, C^*, D^*)}{\partial T^*} & \frac{\partial g(T^*, C^*, D^*)}{\partial C^*} & \frac{\partial g(T^*, C^*, D^*)}{\partial D^*} \\ \frac{\partial h(T^*, C^*, D^*)}{\partial T^*} & \frac{\partial h(T^*, C^*, D^*)}{\partial C^*} & \frac{\partial h(T^*, C^*, D^*)}{\partial D^*} \end{bmatrix} \Rightarrow J \\ &= \begin{bmatrix} -\gamma - \phi C^* - \alpha(\beta T^* - 1) - \alpha\beta T^* & -\phi T^* & 0 \\ \nu - \eta C^* & -\kappa - \eta T^* & 0 \\ \sigma D^* & -\rho D^* & \sigma T^* - \omega - \rho C^* \end{bmatrix}. \end{aligned} \tag{34}$$

We have

$$\Rightarrow J - \lambda I = \begin{bmatrix} -\gamma - \phi C^* - \alpha(\beta T^* - 1) - \alpha\beta T^* - \lambda & -\phi T^* & 0 \\ \nu - \eta C^* & -\kappa - \eta T^* - \lambda & 0 \\ \sigma D^* & -\rho D^* & \sigma T^* - \omega - \rho C^* - \lambda \end{bmatrix}. \tag{35}$$

The characteristic equation is  $|J - \lambda I| = 0$

$$\begin{aligned} \Rightarrow & (-\omega - \rho C^* + \sigma T^* - \lambda) [\lambda^2 + \lambda(\gamma - \alpha + \kappa + \phi C^* + \eta T^* \\ & + 2\alpha\beta T^*) + \kappa(\gamma - \alpha) + \eta T^*(\gamma - \alpha) + \phi\nu T^* + \phi\kappa C^* \\ & + 2\alpha\beta\kappa T^* + 2\alpha\beta\eta T^{*2}] = 0, \end{aligned} \tag{36}$$

where

$$\begin{aligned} \beta_1 &= \gamma - \alpha + \kappa + \phi C^* + \eta T^* + 2\alpha\beta T^*, \\ \beta_2 &= \kappa(\gamma - \alpha) + \eta T^*(\gamma - \alpha) + \phi\nu T^* + \phi\kappa C^* + 2\alpha\beta\kappa T^* + 2\alpha\beta\eta T^{*2}. \end{aligned} \tag{37}$$

The eigenvalue  $\lambda = -\omega - \rho C^* + \sigma T^*$  will be negative if  $\omega + \rho C^* > \sigma T^*$ . If  $\gamma > \alpha$ , then  $\beta_1$  and  $\beta_2$  will have the same sign. Since  $\beta_1$  and  $\beta_2$  are the same sign, according to the Routh-Hurwitz criterion, the other eigenvalues have a negative real part. So, the equilibrium point  $E_1(T^*, C^*, D^*)$  is stable.  $\square$

Alternatively, at the equilibrium point  $E_1(T^*, C^*, D^*)$ , we have basic reproduction number  $R_0 = \alpha / (2\alpha\beta T^* + \gamma + \phi C^*)$ .

One of the eigenvalues is  $\lambda = -\omega - \rho C^* + \sigma T^*$  which is negative if  $(\omega + \rho C^*) > \sigma T^*$ .  $\beta_1$  is positive if  $\gamma > \alpha$ , and we have

$$\begin{aligned} \beta_2 &= \kappa(\gamma - \alpha) + \eta T^*(\gamma - \alpha) + \phi\nu T^* + \phi\kappa C^* + 2\alpha\beta\kappa T^* \\ &+ 2\alpha\beta\eta T^{*2} \Rightarrow \beta_2 = \kappa\alpha \left( \frac{\gamma + \phi C^* + 2\alpha\beta T^*}{\alpha} - 1 \right) \\ &+ \eta T^*(\gamma - \alpha) + \phi\nu T^* + 2\alpha\beta\eta T^*, \\ \Rightarrow \beta_2 &= \kappa\alpha \left( \frac{1}{R_0} - 1 \right) + \eta T^*(\gamma - \alpha) + \phi\nu T^* + 2\alpha\beta\eta T^*. \end{aligned} \tag{38}$$

Hence,  $\beta_1$  and  $\beta_2$  will have the same sign if  $R_0 < 1$ ,  $\gamma > \alpha$ , and  $\omega + \rho C^* > \sigma T^*$ . Therefore, the eigenvalues will be negative, and the system will be stable at the equilibrium  $E_1(T^*, C^*, D^*)$ .

*2.1.6. Characteristics of States for Equilibrium Values with respect to  $\alpha$ .* We will discuss the characterization of the equilibrium values of tumor cells, CD8+ T cells, and dendritic cells with respect to  $\alpha$ .

From equations (18)-(20), we can obtain two functions of  $T^*$ ,  $D^*$ , and  $\alpha$  as follows:

$$\begin{aligned} f(T^*, D^*, \alpha) &= \alpha T^*(1 - \beta T^*) - \gamma T^* - \phi T^* \frac{\nu T^*}{\eta T^* + \kappa}, \\ g(T^*, D^*, \alpha) &= \mu + \sigma D^* T^* - \rho D^* \frac{\nu T^*}{\eta T^* + \kappa} - \omega D^*, \\ \frac{dT^*}{d\alpha} &= \frac{\begin{vmatrix} \partial f / \partial D^* & \partial f / \partial \alpha \\ \partial g / \partial D^* & \partial g / \partial \alpha \end{vmatrix}}{\begin{vmatrix} \partial f / \partial T^* & \partial f / \partial D^* \\ \partial g / \partial T^* & \partial g / \partial D^* \end{vmatrix}} = \frac{((\partial f / \partial D^*)(\partial g / \partial \alpha)) - ((\partial f / \partial \alpha)(\partial g / \partial D^*))}{((\partial f / \partial T^*)(\partial g / \partial D^*)) - ((\partial f / \partial D^*)(\partial g / \partial T^*))} \Rightarrow \frac{dT^*}{d\alpha} \\ &= \frac{2\phi\nu T^*}{\kappa + \eta T^*} + \alpha\beta T^* - \frac{T(\beta T^* - 1)}{\gamma + \alpha(\beta T^* - 1)} - \frac{\phi\nu\eta T^{*2}}{(\kappa + \eta T^*)^2} \Rightarrow \frac{dT^*}{d\alpha} \\ &= \frac{2\phi\nu T^*}{\kappa + \eta T^*} + \alpha\beta T^* + \frac{T^*(1 - \beta T^*)}{\gamma - \alpha(1 - \beta T^*)} - \frac{\phi\nu\eta T^{*2}}{(\kappa + \eta T^*)^2} \Rightarrow \frac{dT^*}{d\alpha} \\ &= \alpha\beta T^* + \frac{T^*(1 - \beta T^*)}{\gamma - \alpha(1 - \beta T^*)} + \frac{2\phi\nu T^*(\kappa + \eta T^*) - \phi\nu\eta T^{*2}}{(\kappa + \eta T^*)^2} \Rightarrow \frac{dT^*}{d\alpha} \\ &= \alpha\beta T^* + \frac{T^*(1 - \beta T^*)}{\gamma - \alpha(1 - \beta T^*)} + \frac{2\phi\nu\kappa T^* + 2\phi\nu\eta T^{*2} - \phi\nu\eta T^{*2}}{(\kappa + \eta T^*)^2} \Rightarrow \frac{dT^*}{d\alpha} \\ &= \alpha\beta T^* + \frac{T^*(1 - \beta T^*)}{\gamma - \alpha(1 - \beta T^*)} + \frac{2\phi\nu\kappa T^* + \phi\nu\eta T^{*2}}{(\kappa + \eta T^*)^2}. \end{aligned} \tag{39}$$

Applying the condition  $\gamma > \alpha$  and  $\beta T < 1$ , third term will be positive.

So, we can obtain  $dT/d\alpha > 0$  that means  $T^* > 0$  when  $\alpha > 0$ .

$$\begin{aligned} \frac{dD^*}{d\alpha} &= \frac{\begin{vmatrix} \partial f/\partial\alpha & \partial f/\partial T^* \\ \partial g/\partial\alpha & \partial g/\partial T^* \end{vmatrix}}{\begin{vmatrix} \partial f/\partial T^* & \partial f/\partial D^* \\ \partial g/\partial T^* & \partial g/\partial D^* \end{vmatrix}} = \frac{((\partial f/\partial\alpha)(\partial g/\partial T^*) - (\partial f/\partial T^*)(\partial g/\partial\alpha))}{((\partial f/\partial T^*)(\partial g/\partial D^*) - (\partial f/\partial D^*)(\partial g/\partial T^*))} \Rightarrow \frac{dD^*}{d\alpha} \\ &= \frac{-\left[T^*(\beta T^* - 1)\left(\sigma D^* - (\nu\rho D^*/(\kappa + \eta T^*)) + (\nu\eta\rho D^* T^*/(\kappa + \eta T^*)^2)\right)\right]}{(\omega - \sigma T^* + (\nu\rho T^*/(\kappa + \eta T^*)))\left(\gamma + \alpha(\beta T^* - 1) + \alpha\beta T^* + (2\nu\phi T^*/(\kappa + \eta T^*)) - (\phi\nu\eta T^{*2}/(\kappa + \eta T^*)^2)\right)} \Rightarrow \frac{dD^*}{d\alpha} \\ &= \frac{T^*(1 - \beta T^*)\left(\sigma D^* - (\nu\rho D^*/(\kappa + \eta T^*)) + (\nu\eta\rho D^* T^*/(\kappa + \eta T^*)^2)\right)}{(\omega - \sigma T^* + (\nu\rho T^*/(\kappa + \eta T^*)))\left(\gamma + \alpha(\beta T^* - 1) + \alpha\beta T^* + (2\nu\phi T^*/(\kappa + \eta T^*)) - (\phi\nu\eta T^{*2}/(\kappa + \eta T^*)^2)\right)} \Rightarrow \frac{dD^*}{d\alpha} \\ &= \frac{T^*(1 - \beta T^*)\left((\sigma\kappa^2 D^* + 2\sigma\kappa\eta D^* T^* + \sigma\eta^2 D^* T^{*2} - \nu\rho\kappa D^*)/(\kappa + \eta T^*)^2\right)}{(\omega - \sigma T^* + (\nu\rho T^*/(\kappa + \eta T^*)))\left(\gamma + \alpha(\beta T^* - 1) + \alpha\beta T^* + (2\nu\phi T^*/(\kappa + \eta T^*)) - (\phi\nu\eta T^{*2}/(\kappa + \eta T^*)^2)\right)}. \end{aligned} \tag{40}$$

Applying the condition  $\beta T^* < 1$ ,  $\gamma > \alpha$ ,  $\sigma\kappa > \nu\rho$ , and  $\omega > \sigma T$ , we can obtain  $dD^*/d\alpha > 0$  that indicates  $D^*$  is increasing when  $\alpha$  is increasing.

$dC^*/d\alpha > 0$  since  $dT^*/d\alpha > 0$ . That indicates that  $C^*$  is increasing when  $\alpha$  is increasing.

**2.1.7. Nature of Tumor Cells When CD8+ T Cells Are Nondecreasing.** For finding nature of tumor cells when CD8 + T cells are nondecreasing, we consider a Holling type-II functional response  $C(t) = \phi_1 t/(1 + \phi_2 t)$ , and substituting this in Section 2.1.2, we obtain

$$\frac{dT}{dt} = \alpha T(1 - \beta T) - \gamma T - \phi T \frac{\phi_1 t}{1 + \phi_2 t}. \tag{41}$$

Now putting right equals of first derivative,

$$\alpha T(1 - \beta T) - \gamma T - \phi T \frac{\phi_1 t}{1 + \phi_2 t} = 0. \tag{42}$$

From the above equation, we get the solution,  $T(t) = 0$  and  $T(t) = 1/\beta - \gamma/\alpha\gamma - \phi\phi_1 t/(1 + \phi_2 t)\alpha\beta$ .

The second derivative is

$$\frac{d^2 T}{dt^2} = -\frac{\phi\phi_1 T}{(1 + \phi_2 t)^2}. \tag{43}$$

Putting the values of  $T$ , we get

$$\begin{aligned} \frac{d^2 T}{dt^2} &= 0, \\ \frac{d^2 T}{dt^2} &= \frac{\phi\phi_1}{\alpha\beta(1 + \phi_2 t)^3} (\gamma + \phi_2 \gamma t + \phi \gamma t - \alpha - \alpha\phi_2 t). \end{aligned} \tag{44}$$

For maximum value, we have  $d^2 T/dt^2 < 0$ .

Therefore,  $t < (\alpha - \gamma)/(\phi_2 \gamma + \phi\phi_1 - \alpha\phi_2)$ . Since  $\gamma > \alpha$ , so denominator will be positive and the numerator will be negative which indicates that tumor cells will have maximum value for the previous day, but in the first quadrant, it does not have any maximum value. Hence, tumor cells do not have maximum value, and it can be concluded that the number of tumor cells will not exceed the initial value of tumor cells if CD8+ T cells are nondecreasing. When immunotherapy and chemotherapy are used, CD8+ T cells will not be declining. With the help of these treatments, the immune system will be strengthened and better able to combat cancerous cells. Also, some healthy foods help to boost the immune system.

**2.1.8. Convergence of Tumor Cells When CD8+ T Cells Are Constant.** When the number of CD8+ T cells is constant, we use  $C = C_c$  to determine the convergence of tumor cells. By using immunotherapy, CD8+ T cells can be made constant. We get by substituting this constant value into Section 2.1.2,

$$\begin{aligned}
 \frac{dT}{dt} &= \alpha T(1 - \beta T) - \gamma T - \phi C_c T \Rightarrow \frac{dT}{dt} \\
 &= T(\alpha - \alpha\beta T - \gamma - \phi C_c) \Rightarrow \frac{dT}{T(\alpha - \alpha\beta T - \gamma - \phi C_c)} \\
 &= dt \Rightarrow \frac{1}{(\alpha - \gamma - \phi C_c)} \left( \frac{1}{T} + \frac{\alpha\beta}{\alpha - \alpha\beta T - \gamma - \phi C_c} \right) \\
 &= dt \Rightarrow \frac{1}{(\alpha - \gamma - \phi C_c)} \{ \ln T - \ln \alpha - \alpha\beta T - \gamma - \phi C_c \} \\
 &= t + k \Rightarrow \frac{\alpha - \alpha\beta T - \gamma - \phi C_c}{T} = e^{t(\gamma + \phi C_c - \alpha)} e^{-k(\alpha - \gamma - \phi C_c)} \Rightarrow T \\
 &= \frac{\alpha - \gamma - \phi C_c}{e^{t(\gamma + \phi C_c - \alpha)} e^{-k(\alpha - \gamma - \phi C_c)} + \alpha\beta}.
 \end{aligned} \tag{45}$$

By taking limit  $t \rightarrow \infty$ , we obtain

$$\lim_{t \rightarrow \infty} T(t) = 0. \tag{46}$$

So, tumor cells converge to zero when the number of CD8+ T cells remains constant. The number of CD8+ T cells will remain constant regardless of the number of tumor cells. As a consequence, CD8+ T cells will continue to destroy cancer cells without diminishing, and tumor cells will converge to zero over a period of time.

*2.1.9. Convergence of CD8+ T Cells When Tumor Cells are Constant.* We use the number of tumor cells as a constant to find the convergence of CD8+ T cells. For making tumor cells constant, surgery or other treatments can be applied. So, we take  $T = T_c$  and substitute it into Section 2.1.2, yielding

$$\begin{aligned}
 \frac{dC}{dt} &= \nu T_c - \eta C T_c - \kappa C \Rightarrow \frac{dC}{dt} \\
 &= \nu T_c - (\eta T_c + \kappa) C \Rightarrow \frac{dC}{dt} + (\eta T_c + \kappa) C \\
 &= \nu T_c.
 \end{aligned} \tag{47}$$

By taking limit  $t \rightarrow \infty$ , we obtain

$$\lim_{t \rightarrow +\infty} C(t) = \frac{\nu T_c}{\eta T_c + \kappa}. \tag{48}$$

This means that as the number of tumor cells grows, so will the number of CD8+ T cells. Because in the presence of tumor cells, dendritic cells become active and stimulate CD8 + T lymphocytes. When CD8+ T cells destroy cancer cells, the number of tumor cells decreases, and the CD8+ T cells become inactive. As a result, CD8+ T lymphocytes will decline as tumor cells decline.

*2.1.10. Relation among State Variables.* Finally, to discuss the qualitative behavior of our model, we simulated the model to obtain phase portraits. The nonlinear behavior is shown in Figure 1.

Figure 1(a) depicts the relationship between CD8+ T cells and tumor cells. The initial point, the number of

CD8+ T cells, and the number of tumor cells were 500 and 10,000, respectively. Then, CD8+ T cells start to increase to compensate for the tumor cell increase. When the number of tumor cells reaches its peak at 130 days, tumor cells begin to decrease, but CD8+ T cells are still increasing. When the number of CD8+ T cells reaches its peak at 160 days, then they start to decline (see Figure 2(a)). With the decrease of CD8+ T cells, tumor cells begin to increase again.

Dendritic cells proliferate rapidly in response to tumor cell development in the human body, as shown in Figure 1(b). After a period of time, dendritic cells continue to increase slowly in response to tumor cell growth. When the number of tumor cells reaches a critical level, the number of tumor cells and dendritic cells both begins to decline.

Figure 1(c) which is drawn for different sets of initial values represents the convergence of state variables.

*2.2. Numerical Simulations.* For analyzing mathematical model, we have used MATLAB (R2018a). The system has been solved by the Runge-Kutta method using the values of parameters from Table 1 which was taken from [7, 9, 15].

In human body, normal range of CD8+ T cells is 150 to 1000 per  $\text{mm}^3$  [25], so the mean of this range  $C(0) = 500$  cells/ $\text{mm}^3$  is assumed as initial value of CD8+ T cells. Furthermore, the mean of normal range of dendritic cells is  $10 \times 10^6$  cells/L [26]. Hence,  $D(0) = 10$  cells/ $\text{mm}^3$  is considered as initial value of dendritic cells. Since we are showing the effect of tumor cells for first 1 year so,  $T(0) = 10000$  is taken as initial value of tumor cells and graphical representation displays the behavior of the cells for 365 days.

Firstly, in Figure 2(a), the solution of the system of non-linear ordinary differential equation has been illustrated which shows the behavior of tumor cells and immune cells. Here, tumor cells are increasing gradually up to 60 days, and the number of cells reaches to  $13 \times 10^4$ . From day 61, behavior of tumor cells is significantly changed as tumor cells start to increase rapidly and attain peak at around 130 days with the number of cells  $20 \times 10^5$  approximately. Then, it starts to decrease rapidly. After that, tumor cells again make an increase and decrease like a wave as shown in the figure but amplitude is lower than previous wave.

At the same time, CD8+ T cells are increasing slowly till 60 days and a number of cells become almost  $3 \times 10^4$ . From day 61, CD8+ T is showing a rapid growth and obtains its peak at around 160 days with the number of cells  $7 \times 10^5$  approximately. Then, it begins to reduce slowly and again make an increase where increasing and decreasing are not as higher as previous increase and decrease. From the dynamics of dendritic cells, it can be seen that from first day to 80 days, changes of dendritic cells are not noticeable. After day 80, cells are changing significantly up to 200 days. After that, a number of cells become almost unchanged.

Figure 2(b) shows how tumor cells alter when the tumor growth rate  $\alpha$  changes. There is no effect of variations in  $\alpha$  on number of tumor cells up to 40 days. Tumor cells rise after 40 days as the tumor growth rate  $\alpha$  increases, and the peak gets larger. Variations in  $\alpha$  have no effect on tumor cells from day 142 to 152, and then, they decrease somewhat as  $\alpha$



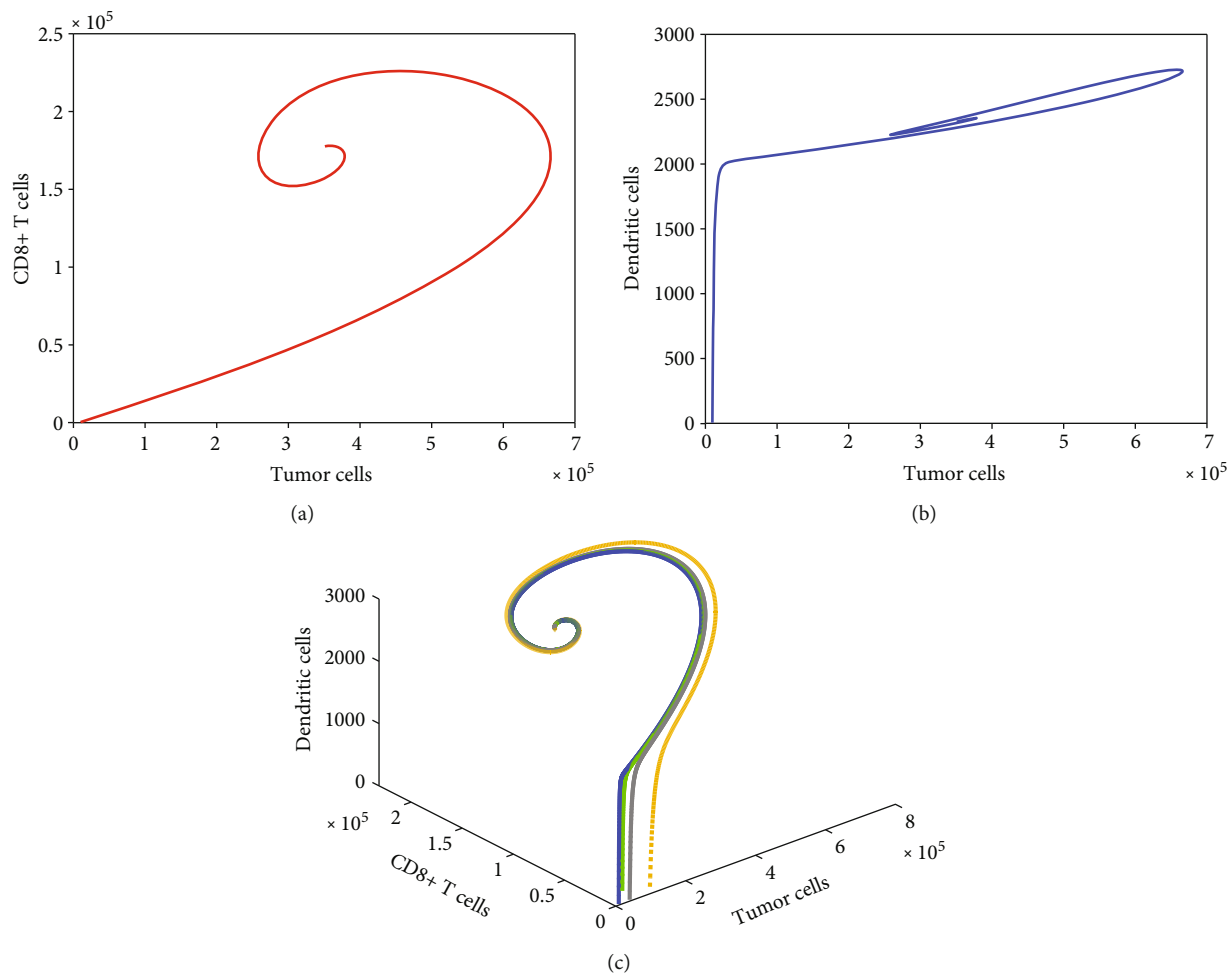


FIGURE 1: (a) Relation between tumor cells  $T(t)$  and CD8+ T cells  $C(t)$ . (b) Relation between tumor cells  $T(t)$  and dendritic cells  $D(t)$ . (c) For different sets of initial values, state variables are converging.

rises. The number of cells stays constant for various values of  $\alpha$  from day 205 to 215 and then starts to climb as  $\alpha$  rises.

Figure 2(c) illustrates the effect of increasing the tumor growth rate  $\alpha$  on CD8+ T cells. From day one to day 50, the number of cells stays constant, and there is no impact of increasing  $\alpha$  on CD8+ T cells. For an increase in tumor growth rate  $\alpha$ , the number of tumor cells increases after day 50. The number of cells becomes invariant for fluctuations in  $\alpha$  from day 200 to 240 and thereafter rises with increases in  $\alpha$ .

Variations in  $\alpha$  have little effect on dendritic cells, as seen in Figure 2(d). However, owing to an increase in  $\alpha$ , they are fluctuated from day 80 to 190, and the maximum number of cells rises.

Variations in  $\nu$  had no influence on the quantity of tumor cells from day 1 to day 80, as shown in Figure 3(a). After that, tumor cells vary significantly for variation of activation rate of CD8+ T cells  $\nu$  because of dendritic cells.

Figure 3(b) shows that the number of CD8+ T cells remains constant from day 1 to day 30 regardless of  $\nu$  fluctuation. After day 30, the number of CD8+ T cells begins to rise modestly in response to a small increase in  $\nu$ . For any value of  $\nu$ , the number of cells becomes the same at around 160 days and then decreases as the value of  $\nu$

increases. At 260 days, the number of cells becomes constant for whatever value of  $\nu$  and then begins to rise gradually.

From Figure 3(c), it can be seen that there is no effect on number of dendritic cells for the variation of  $\nu$  from day 1 to day 70. Following that, as the value of  $\nu$  climbs, the number of dendritic cells falls, reaching a new peak for each value of  $\nu$ .

Figure 4(a) shows that the number of tumor cells remains constant from day 1 to day 50 regardless of the tumor cell killing rate  $\phi$  by CD8+ T cells. The number of tumor cells grows as the value of  $\phi$  increases.

We can see from Figure 4(b) that the adjustment in  $\phi$  has no effect on CD8+ T cells from day 1 to day 70. The number of cells then begins to shift considerably in response to variations in  $\phi$ .

Figure 4(c) demonstrates that for the first 80 days, dendritic cells stay unaltered in response to changes in  $\phi$ , but after 80 days, it begins to shift somewhat. When the value of  $\phi$  varies, the peak of dendritic cells shifts.

2.3. Results and Discussion. Lung cancer is the second most prevalent malignancy in both men and women among all

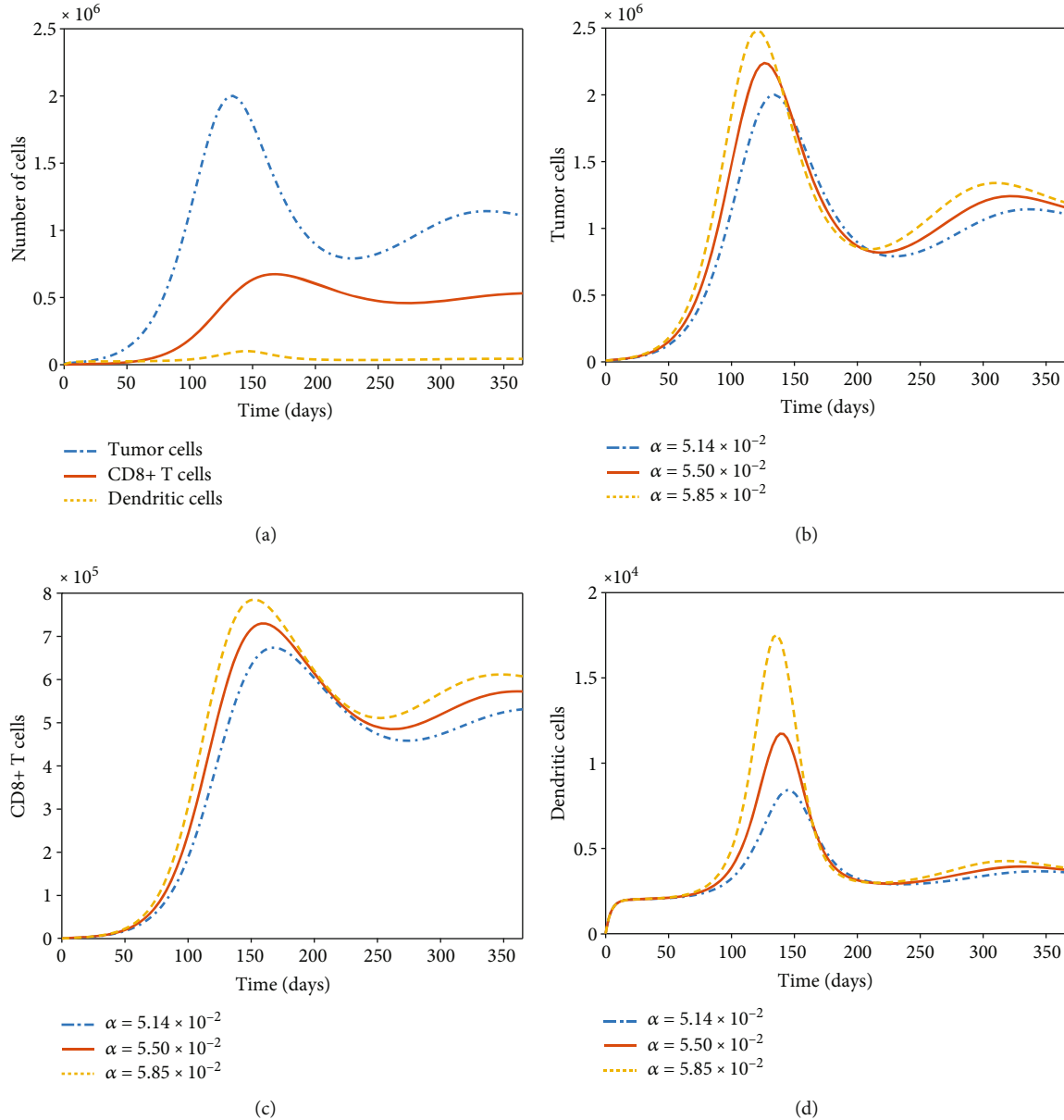


FIGURE 2: (a) Dynamics of tumor cells, CD8+ T cells, and dendritic cells. For visible of dendritic cells, scaling was applied. (b) Tumor cells are increasing gradually for increase of  $\alpha$ . (c) For the increase of tumor growth rate  $\alpha$ , CD8+ T cells are gradually increasing. (d) The peak of dendritic cells is increasing rapidly for increase of tumor growth rate  $\alpha$ .

forms of cancer. Overall, in man’s lifetime, lung cancer is around 1 in 15 cancer patients. Women, on the other hand, account for around one in every fifteen cancer patients.

In lung cancer, initially tumor cells start to increase and stimulate dendritic cells. Then, dendritic cells activate CD8+ T cells. As a consequence, CD8+ T cells grow as much as dendritic cells rise and dendritic cells increase as much as tumor cells increase. After a particular amount of time, tumor cells start to decline due to dendritic cells and CD8+ T cells (see Figure 2(a)). When a number of dendritic cells and CD8+ T cells start to be inactive, so tumor cells again increase.

For a minor fluctuation of  $\alpha$ , the quantity of tumor cells is not altering significantly. There is no need to fear if tumor

growth rate  $\alpha$  of a lung cancer patient varies. Because after a set period of time, the number of tumor cells will be similar for whatever growing rate of tumor (see Figure 2(b)). Since a minor variation in tumor growth rate  $\alpha$  cannot produce a major change in number of tumor cells, thus for this variation, dendritic cells will not be influenced considerably (see Figure 2(c)), because dendritic cells are depending on quantity of tumor cells. As a result, the number of CD8+ T cells will not be changed significantly for the change of  $\alpha$  (see Figure 2(d)).

The number of CD8+ T cells increases as  $\nu$  rises (see Figure 3(b)). We know that CD8+ T cells are immune cells that kill tumor cells; they are useful in the battle against tumor cells. As a result, the number of tumor cells reduces

TABLE 1: Parameter values and their descriptions.

Descriptions of the parameter	Notations	Values
Tumor growth rate	$\alpha$	$5.14 \times 10^{-2} \text{ day}^{-1}$
$1/\beta$ is carrying capacity	$\beta$	$1.02 \times 10^{-9}$
Tumor cells kill by dendritic cells	$\gamma$	$1 \times 10^{-6} \text{ day}^{-1}$
Tumor cells killing rate by CD8+ T cells	$\phi$	$1 \times 10^{-7} \text{ cells}^{-1} \text{ mm}^3 \text{ day}^{-1}$
Activation rate of CD8+ T cells for the interaction of dendritic cells and tumor cells	$\nu$	$0.01 \text{ cells mm}^{-3} \text{ day}^{-1}$
Inactivation rate of CD8+ T cells by tumor cells	$\eta$	$3.42 \times 10^{-10} \text{ day}^{-1}$
Death rate of CD8+ T cells	$\kappa$	$2 \times 10^{-2} \text{ day}^{-1}$
Constant source of dendritic cells	$\mu$	$4.8 \times 10^2 \text{ cells mm}^{-3} \text{ day}^{-1}$
Proliferation rate of dendritic cells due to tumor cells	$\sigma$	$1 \times 10^{-7} \text{ day}^{-1}$
Inactivation rate of dendritic cells by CD8+ T cells	$\rho$	$1 \times 10^{-8} \text{ cells}^{-1} \text{ mm}^3 \text{ day}^{-1}$
Death rate of dendritic cells	$\omega$	$2.4 \times 10^{-1} \text{ day}^{-1}$

as the number of CD8+ T cells grows (see Figure 3(a)). Dendritic cells are activated for tumor cells. So, they begin to diminish when the number of tumor cells decreases with the growth of  $\nu$  (see Figure 3(c)).

Since  $\phi$  represents the decreasing rate of tumor cells by CD8+ T cells, the number of tumor cells reduces as  $\phi$  rises (see Figure 4(a)). The amount of tumor cells determines the activation of dendritic cells. As a result, dendritic cells will reduce in quantity as tumor cells decrease (see Figure 4(c)), and the activation of CD8+ T cells will be dependent on the amount of dendritic cells. As a consequence, the number of CD8+ T cells will reduce as the number of dendritic cells diminishes (see Figure 4(b)).

According to [9], dendritic cells become active in the presence of tumor cells. Then, they will activate CD8+ T cells. CD8+ T cells fight against tumor cells. When CD8+ T cells become active, they start to fight against tumor cells. A small amount of dendritic cells also kills cancer cells. That is similar to our findings.

### 3. Treatment of Non-Small-Cell Lung Cancer: Modeling Approach Using Surgery and Chemotherapy

Lung cancer is the most frequent cancer among males in terms of incidence and death, and it is the third most common disease among women in terms of incidence and mortality, behind only breast cancer. Women's lung cancer death rates have been growing for decades and are just now starting to stabilize, in contrast to men's lung cancer mortality rates, which have been dropping for more than 20 years [27]. If lung cancer is discovered, more tests are performed to determine the extent of the disease's spread throughout the lungs, lymph nodes, and the rest of the body. This is referred to as staging. The kind and stage of lung cancer determine the treatment options available to patient. There are two types of lung cancer. First one is small-cell lung cancer and second one is non-small-cell lung cancer. We are using surgery and chemo-

therapy as a first-line treatment option for non-small-cell lung cancer in stages I and II [28].

*3.1. Formulation of the Mathematical Model.* To formulate a mathematical model, we assume that some cancer cells may be left behind following surgery. As a result, cancer may resurface. Chemotherapy following surgery can assist to reduce the chance of non-small-cell lung cancer (NSCLC) recurrence in patients with early stage. We assume that 5% of tumor cells remain after surgery and 1% remain after chemotherapy, and surgery is performed after 100 days of tumor growth. Chemotherapy is usually started within eight weeks following surgery, so we will start on the 128th day. We also assume that 2% of CD8+ T cells and dendritic cells will be destroyed by chemotherapy. We consider that chemotherapy works instantly for our numerical solution which is the limitation of our model.

Hence, here is our mathematical model for treatment of NSCLC:

$$\begin{aligned}
 \frac{dT}{dt} &= \alpha T(1 - \beta T) - \gamma T - \phi CT - \xi_{100} T - \psi_{128} T, \\
 \frac{dC}{dt} &= \nu T - \eta CT - \kappa C - \tau_{128} C, \\
 \frac{dD}{dt} &= \mu + \sigma DT - \rho CD - \omega D - \zeta_{128} D,
 \end{aligned} \tag{49}$$

where the destruction rates of tumor cells due to surgery on day 100 and chemotherapy on day 128 are denoted by  $\xi_{100}$  and  $\psi_{128}$ , respectively.  $\tau_{128}$  and  $\zeta_{128}$  represent the killing rates of CD8+ T cells and dendritic cells by chemotherapy on day 128, respectively.

*3.2. Numerical Simulations.* The impact of various treatment approaches on tumor cells is shown in Figure 5. Immune cells are unable to suppress tumor development in the absence of any treatment options.

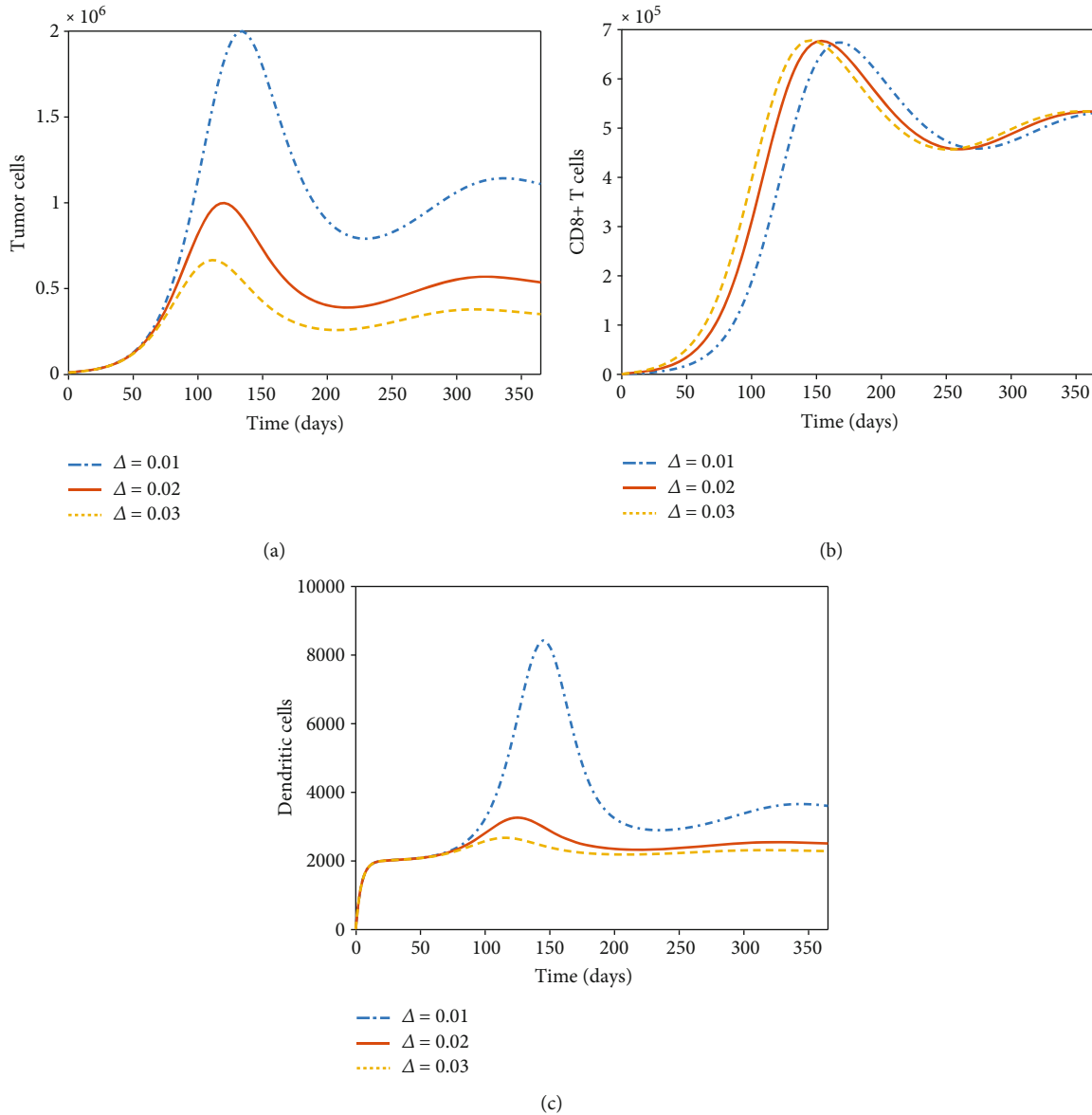


FIGURE 3: (a) Tumor cells are changing considerably for variation of  $\nu$ . (b) CD8+ T cells are slightly increasing for little rise of  $\nu$ . (c) Peak of dendritic cells is changing because of variation of  $\nu$ .

Tumor cells decrease in the presence of a large number of CD8+ T cells and dendritic cells and then rise when these immune cells decline. When surgery is performed on the 100th day, the number of tumor cells immediately decreases and 95% of them are removed. If no therapy is given without surgery, the remaining 5% of tumor cells develop rapidly and act like tumors that have not been treated. When the first round of chemotherapy is given on day 128 following surgery, the remaining tumor cells rapidly decline. However, 1% of tumor cells persist in the human body after surgery and the first chemotherapy dosage. As a consequence, tumors begin to be developed once again. If a patient misses the first dosage of chemotherapy after surgery for whatever reason and takes the second dose, 5 percent of tumor cells grow fast after surgery and abruptly decline after 156 days

due to the second dose of chemotherapy, and then, they begin to grow again. Patients who take both dosages feel better than those who just take one. Under this situation, tumor cells are in control up to 250 days and then develop fast. Following surgery, we use three rounds of chemotherapy to get the greatest results. This treatment method shows that tumor cells can be controlled for up to 350 days. The doctor will then decide what to do.

Figure 6 shows how CD8+ T cells change as a result of various treatment methods. CD8+ T cells rise without treatment when the number of dendritic cells in the body increases.

When 95 percent of tumor cells are removed by surgery on day 100, the number of CD8+ T cells decreases significantly due to a decrease in dendritic cells. If the patient does not get chemotherapy after surgery, CD8+ T cells will begin to

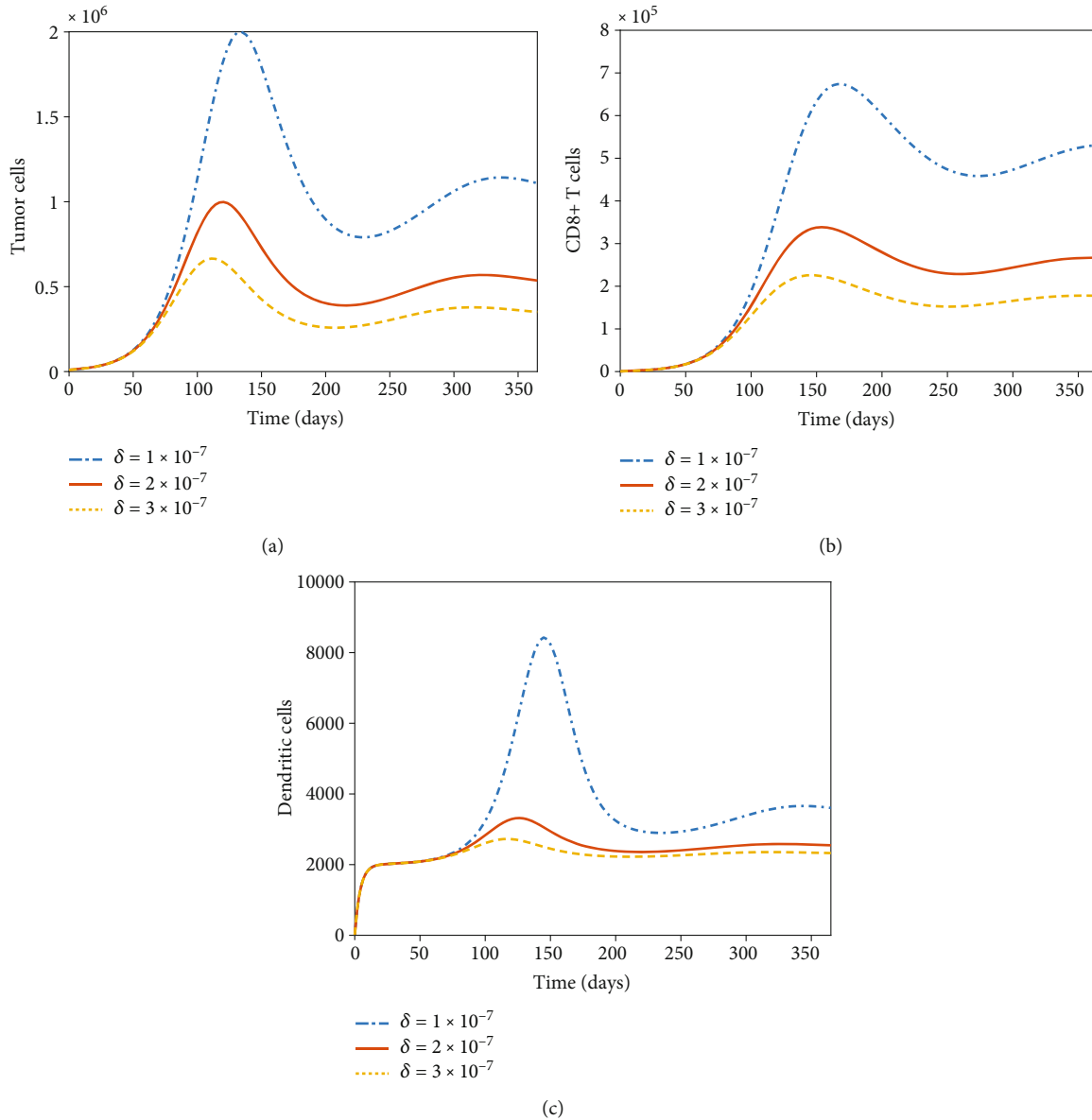


FIGURE 4: (a) For variations in  $\phi$ , tumor cells change dramatically. (b) Variation in  $\phi$  causes CD8+ T cells to change significantly. (c) Because of variations in  $\phi$ , the peak of dendritic cells is altering.

increase and fluctuate again. The decline in CD8+ T cells will remain if he takes his first dose of chemotherapy following surgery because chemotherapy cannot identify cancer cells and fast-growing immune cells, but they will begin to rise after day 225 if the patient does not take any chemotherapy after the first dose. Patients who get a second dosage of chemotherapy after missing the first dose will have fewer CD8+ T cells after surgery than those who received the first dose. If the patient receives both doses of chemotherapy after surgery, his CD8+ T cells will be lower on day 250 than if he receives just one dose, and then, they will begin to increase. The reduction of CD8+ T cells will be continued for up to 350 days if 3 doses of chemotherapy are taken following surgery.

Dendritic cell dynamics are shown in Figure 7 for various treatment methods. Dendritic cells become active when

they come into contact with tumor cells; hence, dendritic cells multiply in proportion to the number of tumor cells. Dendritic cells reduce dramatically on day 100 after surgery, which eliminates 95% of tumor cells, but grow again if the patient receives no additional therapy. If the patient receives his first dosage of chemotherapy after surgery, dendritic cells will decline again on day 128 and then gradually rise. If the patient does not get more therapy, dendritic cells will continue to develop and fluctuate. A patient who misses his first dose and takes a second dose on day 156 will have a dramatic decline in dendritic cells, and if he does not take future doses, he will have fewer dendritic cells from day 150 to 300 than a patient who takes the first dose after surgery. From days 128 to 350, the patient who receives both doses will have fewer dendritic cells than the patient who receives just

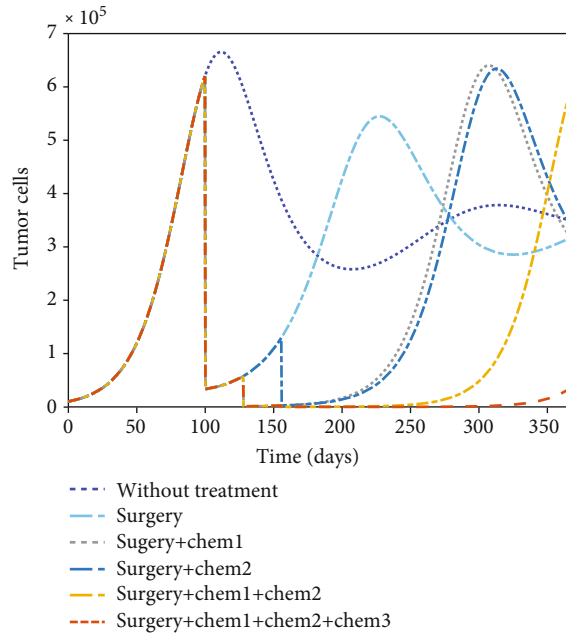


FIGURE 5: Tumor cell dynamics for various treatment approaches.

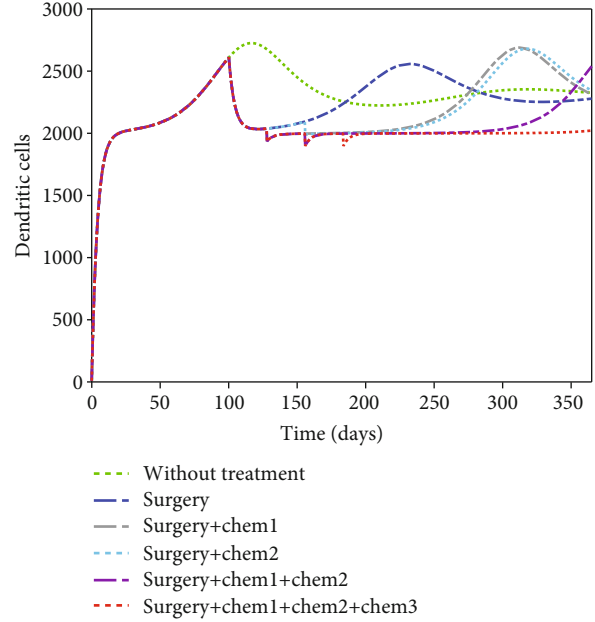


FIGURE 7: Dynamics of dendritic cells for various treatment methods.

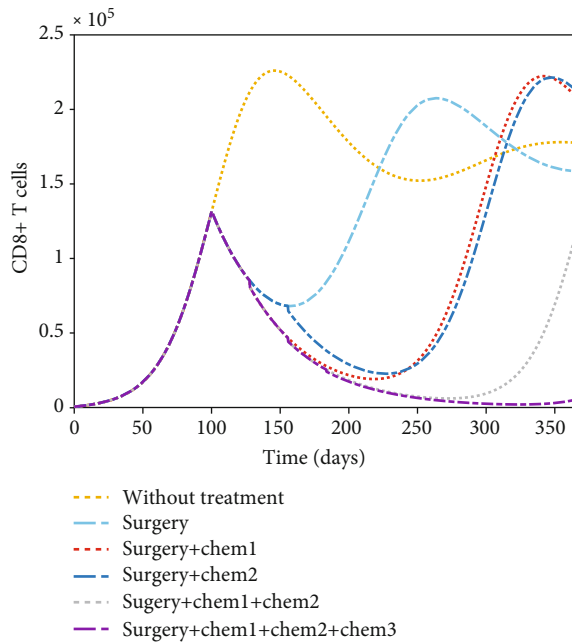


FIGURE 6: Dynamics of CD8+ T cells for various treatment methods.

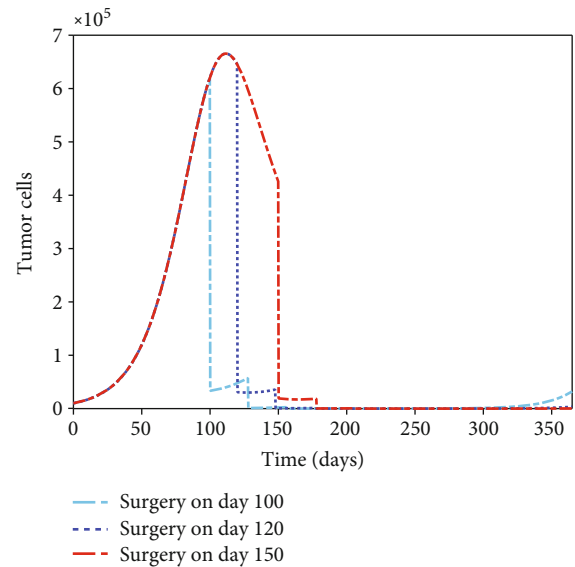


FIGURE 8: Dynamics of tumor cells for starting treatment on days 100, 120, and 150.

one dosage, and the number of cells will be larger if he does not receive more treatment. If the patient has three chemotherapy treatments after surgery, the number of dendritic cells will not rise considerably for up to 365 days.

**3.3. Results and Discussion.** Surgery and chemotherapy are the two most popular treatment options for non-small-cell lung cancer in its early stages. When tumor cells form in the human

body, they quickly multiply, and when surgery is used to eliminate them, they quickly diminish. 5% of tumor cells persist in the patient's lung after surgery. Chemotherapy destroys rapidly developing cells, so if it can be taken after surgery, the outcome will be better. Otherwise, the tumor cells that remain will proliferate anew (see Figure 5).

Dendritic cells stimulate CD8+ T lymphocytes, and tumor cells activate dendritic cells. As a result, when surgery is performed, the number of tumor cells drops dramatically. Dendritic cells diminish as a result of not being able to come

TABLE 2: Toxicity of tumor cells for starting treatment on days 100 and 150.

SL	Treatment strategies	Toxicity of tumor cells (starting treatment on day 100)	Toxicity of tumor cells (starting treatment on day 150)
1	Surgery+chem1+chem2+chem3	$4.8251 \times 10^7$	$6.3816 \times 10^7$
2	Surgery+chem1+chem2	$5.0792 \times 10^7$	$6.4190 \times 10^7$
3	Surgery+chem1	$8.5408 \times 10^7$	$7.6852 \times 10^7$
4	Surgery+chem2	$8.8090 \times 10^7$	$7.8324 \times 10^7$
5	Surgery	$11.5120 \times 10^7$	$11.7840 \times 10^7$

into contact with as many cancer cells as before, and CD8+ T cells fall as a result of dendritic cell depletion. Tumor cells reduce after each dose of chemotherapy, and as a result, CD8+ T cells and dendritic cells drop as well. Chemotherapy is unable to distinguish between fast-growing healthy cells and cancer cells, which contributes to the loss of CD8+ T cells and dendritic cells (see Figures 6 and 7).

Figure 8 depicts the impact of different treatment start days where surgery and three doses of chemotherapy were used as treatment method. The graph demonstrates that if the treatment begins on day 100, the tumor size may be managed for up to 325 days. However, if treatment begins on day 120 or 150, the number of tumor cells can be controlled for a longer period of time than if treatment begins on day 100.

But in this case, the patient may not survive for 120 or 150 days after developing non-small-cell lung cancer because the survival rate of non-small-cell lung cancer is very poor. Furthermore, Table 2 shows that tumor cell toxicity differs depending on the start date of various treatment approaches. Tumor cell toxicity will be lower in a patient who receives three doses of chemotherapy or two doses of chemotherapy after surgery, or in a patient who receives just surgery as a treatment option and begins treatment on day 100, than in a patient who begins treatment on day 150, which indicates that if any of these treatment methods are applied to a patient on day 100, then he will be more beneficial than the patient who starts any of the treatment methods on day 150. Even if the patient begins treatment on day 100, he will not benefit from this treatment if he only receives the first doses of chemotherapy after surgery, or if he skips the first dose and receives a second dose after surgery.

As shown in Table 2, if treatment begins on day 100, three doses of chemotherapy following surgery had the least tumor toxicity of all treatment options. As a result, it might be considered the finest treatment choice. We can observe that the tumor toxicity is growing if this treatment is started after the 100th day. Hence, treatment should begin within 100 days. Otherwise, the cancer has the ability to spread to other parts of the body.

#### 4. Conclusions

Lung cancer is by far the most common cause of cancer mortality in both men and women, accounting for over 25% of all cancer fatalities. It kills more people each year than colon, breast, and prostate cancer combined. We used

mathematical analysis and numerical simulations to analyze our mathematical model.

At first, in our mathematical analysis, basic reproduction represents whether tumor cells will exist or not. Positivity and boundedness analyses reveal that our model's solution is both positive and bounded. Characteristic with respect to  $\alpha$  is showing that equilibrium point is changing for change in tumor growth rate. Then, we have tested convergence of tumor cells and CD8+ T cells by taking CD8+ T cells and tumor cells as constant, respectively, and we observed that tumor cells are converging to zero and CD8+ T cells are increasing for growth of tumor cells.

Then, we performed numerical simulations and discovered that the amount of tumor cells fluctuates depending on how many immune cells are present. When CD8+ T cells and dendritic cells both increase, tumor cells decrease. However, the number of tumor cells outnumbers both CD8+ T cells and dendritic cells. As a result, these immune cells are powerless to stop tumor cells from multiplying. Hence, we used the therapy option to keep this uncontrollable growth under control. The treatment approaches were tested on non-small-cell lung cancer for stages I and II, which is a kind of lung cancer. The treatment choices include surgery and chemotherapy. When three doses of chemotherapy are given after surgery as a treatment option, we have seen an excellent response. Then, for 100, 120, and 150 days, this treatment method was used, and we discovered that the patient should begin his treatment within 100 days. Otherwise, his chances of surviving will be reduced.

Therefore, from our findings, we can conclude that surgery on day 100 is insufficient for recovery, so three doses of chemotherapy following surgery are the best treatment choices with the least tumor toxicity when compared to alternative treatment options.

In the future, we will use best control in our study to demonstrate how tumor cells may be reduced.

#### Data Availability

The article in the text that is cited has all of the data.

#### Disclosure

This manuscript is a part of the unpublished thesis of Md. Ahsan Ullah, Mathematics Discipline, Khulna University, Khulna [29].

## Conflicts of Interest

The authors have no conflict of interest.

## References

- [1] American Cancer Society, "Global cancer facts and figures 4th edition," 2022, April 2021, <https://www.cancer.org/content/dam/cancerorg/research/cancer-facts-and-statistics/global-cancer-facts-and-figures/global-cancer-facts-and-figures-4th-edition.pdf>.
- [2] UICC, "Global cancer data: Globocan 2018," 2021, February 2022, <https://www.uicc.org/news/global-cancer-data-globocan-2018>.
- [3] American Cancer Society, "Lung cancer statistics: how common is lung cancer?," 2022, February 2022, <https://www.cancer.org/cancer/lung-cancer/about/keystatistics.html:text=Lung%20cancer%20is%20by%20far,breast%2C%20and%20prostate%20cancers%20combined>.
- [4] S. M. Hussain, "Comprehensive update on cancer scenario of Bangladesh," *South Asian Journal of Cancer*, vol. 2, no. 4, pp. 279–284, 2013.
- [5] WHO, "Cancer country profile 2020," 2020, January 2022, [https://www.who.int/cancer/country-profiles/BGD\\_2020](https://www.who.int/cancer/country-profiles/BGD_2020).
- [6] L. G. de Pillis, W. Gu, and A. E. Radunskaya, "Mixed immunotherapy and chemotherapy of tumors: modeling, applications and biological interpretations," *Journal of Theoretical Biology*, vol. 238, no. 4, pp. 841–862, 2006.
- [7] L. G. de Pillis, A. E. Radunskaya, and C. L. Wiseman, "A validated mathematical model of cell-mediated immune response to tumor growth," *American Association for Cancer Research*, vol. 65, no. 17, pp. 7950–7958, 2005.
- [8] T. Trisilowati, S. McCue, and D. Mallet, "Numerical solution of an optimal control model of dendritic cell treatment of a growing tumour," *ANZIAM Journal*, vol. 54, no. 2012, pp. 664–680, 2012.
- [9] P. Unni and P. Seshaiyer, "Mathematical modeling, analysis, and simulation of tumor dynamics with drug interventions," *Computational and Mathematical Methods in Medicine*, vol. 2019, Article ID 4079298, 13 pages, 2019.
- [10] D. Kirschner and A. Tsygvintsev, "On the global dynamics of a model for tumor immunotherapy," *Mathematical Biosciences and Engineering*, vol. 6, no. 3, pp. 573–583, 2009.
- [11] D. Kirschner and J. C. Panetta, "Modeling immunotherapy of the tumor - immune interaction," *Journal of Mathematical Biology*, vol. 37, no. 3, pp. 235–252, 1998.
- [12] W. K. Decker, R. F. da Silva, M. H. Sanabria et al., "Cancer immunotherapy: historical perspective of a clinical revolution and emerging preclinical animal models," *Frontiers in Immunology*, vol. 8, p. 829, 2017.
- [13] A. Waldman, J. Fritz, and M. Lenardo, "A guide to cancer immunotherapy: from T cell basic science to clinical practice," *Nature Reviews Immunology*, vol. 20, no. 11, pp. 651–668, 2020.
- [14] K. J. Hiam-Galvez, B. M. Allen, and M. H. Spitzer, "Systemic immunity in cancer," *Nature Reviews. Cancer*, vol. 21, no. 6, pp. 345–359, 2021.
- [15] A. S. Kartono, "Mathematical modeling of the effect of boosting tumor infiltrating lymphocyte in immunotherapy," *Pakistan Journal of Biological Sciences*, vol. 16, no. 20, pp. 1095–1103, 2013.
- [16] L. M. McLane, M. S. Abdel-Hakeem, and E. J. Wherry, "CD8 T cell exhaustion during chronic viral infection and cancer," *Annual Review of Immunology*, vol. 37, no. 1, pp. 457–495, 2019.
- [17] M. Philip and A. Schietinger, "CD8<sup>+</sup> T cell differentiation and dysfunction in cancer," *Nature Reviews. Immunology*, vol. 22, no. 4, pp. 209–223, 2022.
- [18] M. Casiraghi, G. Sedda, E. Del Signore et al., "Surgery for small cell lung cancer: when and how," *Lung Cancer*, vol. 152, pp. 71–77, 2021.
- [19] M. Liang, M. Chen, S. Singh, and S. Singh, "Prognostic nomogram for overall survival in small cell lung cancer patients treated with chemotherapy: a SEER-based retrospective cohort study," *Advances in Therapy*, vol. 39, no. 1, pp. 346–359, 2022.
- [20] C. Chao, D. Di, M. Wang, Y. Liu, B. Wang, and Y. Qian, "Identifying octogenarians with non-small cell lung cancer who could benefit from surgery: a population-based predictive model," *Frontiers in Surgery*, vol. 9, pp. 1–13, 2022.
- [21] H.-S. Li, J.-L. Li, X. Yan et al., "Efficacy of dacomitinib in patients with non-small cell lung cancer carrying complex EGFR mutations: a real-world study," *Journal of Thoracic Disease*, vol. 14, no. 5, pp. 1428–1440, 2022.
- [22] S. Sowole, D. Sangare, A. Ibrahim, and I. A. Paul, "On the existence, uniqueness, stability of solution and numerical simulations of a mathematical model for measles disease," *International Journal of Advances in Mathematics*, vol. 2019, no. 4, pp. 84–111, 2019.
- [23] R. Kiran, S. Tyagi, S. Abbas, M. Roy, and A. Taraphder, "Immunomodulatory role of black tea in the mitigation of cancer induced by inorganic arsenic," *The European Physical Journal Plus*, vol. 135, no. 9, 2020.
- [24] A. Fentie Bezabih, G. Kenassa Edessa, and P. R. Koya, "Mathematical eco-epidemiological model on prey-predator system," *Mathematical Modelling and Applications*, vol. 5, no. 3, pp. 183–190, 2020.
- [25] University of rochester medical center, "Health encyclopedia," February 2022, [https://www.urmc.rochester.edu/encyclopedia/content.aspx?contentTypeid=167&contentid=cd4\\_cd8\\_ratio:text=A%20normal%20CD4%2FCD8%20ratio,you%20may%20not%20have%20HIV](https://www.urmc.rochester.edu/encyclopedia/content.aspx?contentTypeid=167&contentid=cd4_cd8_ratio:text=A%20normal%20CD4%2FCD8%20ratio,you%20may%20not%20have%20HIV).
- [26] D. B. Fearnley, L. F. Whyte, S. A. Carnoutsos, A. H. Cook, and D. N. Hart, "Monitoring human blood dendritic cell numbers in normal individuals and in stem cell transplantation," *Blood*, vol. 93, no. 2, pp. 728–736, 1999.
- [27] M. Mustafa, A. R. J. Azizi, E. L. IIZam, A. Nazirah, S. Sharifa, and S. A. Abbas, "Lung cancer: risk factors, management, and prognosis," *IOSR Journal of Dental and Medical Sciences*, vol. 15, no. 10, pp. 94–101, 2016.
- [28] National Cancer Institute, "Non-small cell lung cancer treatment (PDQ®)—patient version," 2021, February 2022, <https://www.cancer.gov/types/lung/patient/non-small-cell-lungtreatment-pdq-557>.
- [29] M. A. Ullah, *Mathematical Modeling and Analysis on the Effects of Surgery and Chemotherapy on Lung Cancer*, Unpublished Undergraduate Thesis, Mathematics Discipline, Khulna University, 2022.